# Rapid and accurate detection of Escherichia coli growth by fluorescent pH-sensitive organic nanoparticles for high-throughput screening applications.

Yang Si, Chloé Grazon, Gilles Clavier, Rieger Jutta, J.F. Audibert, Bianca Sclavi, Rachel Méallet-Renault

# Rapid and accurate detection of *Escherichia coli* growth by fluorescent pH-sensitive organic nanoparticles for high-throughput screening applications

Yang SI[a,b], Chloé GRAZON[a], Gilles CLAVIER[a], Jutta RIEGER[c], Jean-Frédéric AUDIBERT[a] , Bianca SCLAVI*[b], Rachel MEALLET-RENAULT*[a]

[a] PPSM, CNRS UMR 8531, ENS-Cachan, 61 av President Wilson , 94230, Cachan, France

[b] LBPA, CNRS UMR 8113, ENS-Cachan, 61 av President Wilson , 94230, Cachan, France

[c] UPMC Univ Paris 06, Laboratoire de Chimie des Polymeres (LCP), UMR 7610 94200 IVRY, France

**Corresponding Authors:**

*Rachel Méallet-Renault

Tel : + 33(0)169153128

E-mail : rachel.meallet-renault@u-psud.fr

PPSM, CNRS UMR 8531, ENS-Cachan, 61 av President Wilson, 94230, Cachan, France

Present Address

ISMO, CNRS UMR 8214, Université Paris-Sud, Avenue Jean Perrin, 91400, ORSAY, France

*Bianca Sclavi

Tel : + 33(0)147407677

E-mail : sclavi@lbpa.ens-cachan.fr

LBPA, CNRS UMR 8113, ENS-Cachan, 61 av President Wilson, 94230, Cachan, France

## Abstract

Rapid detection of bacterial growth is an important issue in the food industry and for medical research. Here we present a novel kind of pH-sensitive fluorescent nanoparticles (FANPs) that can be used for the rapid and accurate real-time detection of *Escherichia coli* growth. These organic particles are designed to be non-toxic and highly water-soluble. Here we show that the coupling of pH sensitive fluoresceinamine to the nanoparticles results in an increased sensitivity to changes in pH within a physiologically relevant range that can be used to monitor the presence of live bacteria. In addition, these FANPs do not influence bacterial growth and are stable over several hours in a complex medium and in the presence of bacteria. The use of these FANPs allows for continuous monitoring of bacterial growth via real-time detection over long time scales in small volumes and can thus be used for the screening of a large number of samples for high-throughput applications such as screening for the presence of antibiotic resistant strains.

**Keywords:** bacteria, fluoresceinamine, organic nanoparticles, rapid detection, high-throughput screening (HTS), pH detection

## 1. Introduction

Rapid detection of bacterial growth is important for medical diagnostics to identify bacterial contamination in medical settings (Barker et al., 2010; Palavecino et al., 2006; Washington, 1996) and in the food industry in order to prevent contamination of food, air, and water (Farris et al., 2008; Ko et al., 2010; Wang et al., 2012).

The classic techniques used to detect bacterial growth rely on plating the sample on agar and counting of colonies after 37-48 hours or more; however this is time-consuming and requires large amounts of samples and materials and may miss most types of bacteria (Lazcka et al., 2007; Nayak et al., 2009; Pourciel-Gouzy et al., 2004). Alternative methods have been developed to reduce the amount of time and sample necessary for a reliable measurement, such as the polymerase chain reaction (PCR). Although PCR and its variants can detect bacteria within a relatively short time (Gopinath et al., 2014; Noble and Weisberg, 2005), issues like primer design and PCR-inhibitory effect of complex food matrices, in addition to its high cost, make PCR detection difficult to be a routine procedure (Gunaydin et al., 2007). Another effective method is enzyme-linked immunoabsorbent assay (ELISA). This technology uses an antigen-antibody reaction to detect unique microorganism. Different technologies have

been developed to enhance ELISA measurements (Chunglok et al., 2011; Jain et al., 2012; Seo et al., 2015). These methods are highly sensitive and provide specific detections. However, this approach requires considerable amounts of expensive reactants such as antibodies and a high level of antigen for reliable detection (Mouffouk et al., 2011). Microfluidic devices are also being developed for the rapid detection of small amounts of bacteria (Chang et al., 2015), however they require relatively expensive laboratory instruments and experienced operators. Biosensing methods based on nanostructures have shown great potential for bacteria detection, such as gold nanoparticle for *E.coli* detection (Hassan et al., 2015), magnetic nanoparticles system (Wan et al., 2014), and fluorescent silica nanoparticles (Chen et al., 2015). For these nanostructures, the potential toxicity effect on bacteria is an important issue to be considered (Adams et al., 2006; Wang et al., 2011). Polymeric organic nanoparticles, however, provide a promising platform to solve this problem. Moreover, different functional molecules can easily be immobilized on their surface to enhance their selectivity and sensitivity.

The growth of bacteria is often associated with a decrease in the pH of the growth medium due to a release of acidic metabolites such as acetic acid, lactic acid and $CO_2$ (John et al., 2003; Young et al., 2004). Different kinds of pH sensors have therefore been used to measure the growth of bacteria based on this principle (Agayn and Walt, 1993; Badugu et al., 2008; Wang, F. et al., 2014; Wang, X. et al., 2013). Unfortunately, the useful life-span of these sensors is limited due to photobleaching and instability in a complex medium. More importantly, some dyes were developed for single assay-based measurements and are often unsuitable for real-time detection applications or to accommodate a large number of samples for high-throughput screening.

While high-throughput screening of bacterial growth has been conducted extensively to search for novel compounds with antibacterial activity (Zlitni et al., 2009), such efforts have been limited by the sensitivity and accuracy of bacterial resistance detection. Traditional optical density based (OD) measurements are limited by cells forming chains, clumps, filaments, or aggregates and are difficult to perform in complex growth media which can result in light scattering or absorption and interfere the detection by OD (Chalova et al., 2003; Gasol et al., 1999). Optical density was found to be linearly correlated with culture biomass between 0.01-0.3, but there might be variations depending on the growth phase and at higher densities the OD deviates from linearity (Martens-Habbena and Sass, 2006). Furthermore, OD measurements cannot

distinguish between live, but slow growing, and dead cells. Screening of bacterial metabolism signatures can provide unambiguous evidence of the existence of live bacteria (Huang et al., 2011) and can offer a more reliable and sensitive assay for the presence of live microorganisms and the detection of antibiotic resistant strains.

In this work, we report the synthesis and full characterisation of two highly water-soluble, biocompatible, stable and bright fluoresceinamine-based pH-sensitive nanoparticles. The addition of these nanoparticles to a growth medium containing bacteria allows for a rapid, accurate, reproducible and highly sensitive detection of bacterial growth.

Compared with the existing methods the one described here is based on nanoparticles that are more sensitive and more stable in common growth media, are easily synthesized with at a low cost and can be used in any laboratory without additional expensive instruments or experienced operators. Moreover, these particles allow for continuous monitoring for real-time detection over long time scales and can be used for screening a large number of samples for high-throughput applications.

## 2. Experimental Methods

### 2.1 Materials

Fluoresceinamine, isomer I (Sigma-Aldrich, FA), 1-ethyl-3-(3-dimethylaminopropyl) carbodiimide hydrochloride (>98%, Fluka, EDC), ethanolamine (>99%, Sigma-Aldrich, EtA), acrylic acid (99%, Sigma-Aldrich, AA), poly(ethylene oxide) methyl ether acrylate (Mn=480 g/mol, Sigma-Aldrich, PEOA), 4,4'-azobis(4-cyanopentanoic acid) (Sigma-Aldrich, ACPA), citric acid (99.8%, Carlo Erba), sodium phosphate dibasic dihydrate (>99.5%, Sigma-Aldrich), 2-methyl-2-[(dodecylsulfanylthiocarbonyl)sulfanyl] propanoic acid (> 97%, Strem, TTCA) were used as received. Chloramphenicol, kanamycin, and ampicillin antibiotics were obtained from Sigma-Aldrich and used as received. 2,2'-Azobis(2-methylpropionitrile) (98%, Sigma-Aldrich, AIBN) was recrystallized from chloroform and few drops of petroleum ether. Styrene was distilled under reduced pressure. Deionized water (15MΩ.cm at 20°C) was prepared with a Milli-Q system (Millipore).

### 2.2 Synthesis of fluoresceinamine (FA) fluorescent pH-sensitive nanoparticles

The synthesis process of macroRAFT agents and polystyrene nanoparticle 1 (PSNP1) and polystyrene nanoparticle 2 (PSNP2) are described in Supplemental

Information (S1.1 S1.2 Table S1 Scheme S1). In a typical experiment, 0.3 mL of PSNPs (0.1 mg/mL) obtained above were diluted in 4 mL of distilled water in the dark. In parallel, depending on the number of the AA units, 0.5 (PSNP1) or 1 (PSNP2) equivalents of fluoresceinamine (FA 3.35 or 6.7 mg) were dissolved in 0.4 mL ethanol and the solution was added to the PSNPs solution. The mixture was then stirred at 4°C. A solution of EDC (4 equiv., 15 mg) in water (1 mL) was then added to the previous mixture. After two hours, ethanolamine (2 equiv., 2.3 µL) was added in order to quench the reaction. The mixture was stirred at 4°C overnight in the dark. Finally, the solution was transferred into a cellulose ester dialysis membrane (MWCO: 300 kDa, Spectrapor) and dialyzed against water in the dark for 7 days. Two different fluoresceinamine (FA) based fluorescent nanoparticles were thus obtained: FANP1 and FANP2.

**2.3 pH measurements**

pH measurements were carried by using a glass electrode connected to a PHM210 standard pH meter from Meterlab.

**2.4 Fluorescence spectroscopy**

The UV-visible spectra were measured on a Varian Cary 5000 (Palo Alto, CA USA) double beam spectrometer using 4.5mL BRAND Methacrylate (PMMA) Cuvette**.** Excitation and emission spectra were recorded on a SPEX Fluoromax-3 (Horiba Jobin-Yvon).

**2.5 Screening of bacterial growth in a 96 well plate**

Live *E.coli* bacterial cells (K-12, BW25113) were used for the following experiments. Bacterial cultures were prepared overnight from stock cultures inoculated in Luria Broth (LB) growth medium.

The overnight culture of bacteria was diluted 1:1000 in the Modified M9 minimal growth medium. (Detailed composition of the M9 medium is in Supplemental Information S1.4). 150µL of this bacterial solution were placed in each well of a 96 well Falcon Polystyrene Flat Bottom Plate. Different volumes (from 2 to 10 µl) of the stock FANP1 and FANP2 solutions were added into the *E.coli* solution to reach final concentrations of $8.2 \times 10^{-7}$M, $4.1 \times 10^{-7}$M and $8.2 \times 10^{-8}$M. Each plate contained three repeats of the same concentration. One control with only bacteria and one blank with only the Modified M9 minimal growth medium were also prepared. 70 µL of mineral oil were added to each well in order to avoid evaporation. Samples were incubated in a

plate reader (Perkin Elmer Victor3 1420 Multilabel Plate Counter) at 37°C in the dark. The growth of the cells was monitored every 6 minutes by reading the optical density (OD@600nm). Fluorescence was measured using a F485/14 filter for excitation and a F535/40 filter for emission. The experiments lasted overnight for ten hours.

### 2.6 Real-Time detection of *E.coli*

2.5mL of Modified M9 minimal growth medium with an initial concentration of $2x10^7$ CFU/mL or $3\text{-}6x10^5$ CFU/mL of *E.coli* bacteria was placed inside a 4.5mL BRAND Methacrylate (PMMA) Cuvette**.** Different volumes of FA molecules, FANP1 or FANP2 solutions were added to this *E.coli* suspension to reach a final concentration of $8.2x10^{-7}$M. Two repeats of the same concentration were carried out during each of the experiments.

The samples were incubated at 37°C in the dark. Every 30 minutes the growth of the cells was monitored using a spectrophotometer, Varian Cary 5000 (Palo Alto, CA USA) that reads the optical density (OD@600nm) of the samples compared to a blank of Modified M9 minimal medium. The pH of the samples was measured using a glass electrode. Emission and excitation spectra of the samples were measured on a SPEX Fluoromax-3 (Horiba Jobin-Yvon).

### 2.7 High-through put screening of bacterial growth inhibition by antibiotics

The assay is performed in a 96 well Falcon Polystyrene Flat Bottom Plate as described above. 150μL of a bacterial solution (1:1000 dilution of an overnight culture) were placed in each well. FANP1 and FANP2 solutions were added into the *E.coli* solution to reach final concentrations of $8.2x10^{-8}$M. Three different antibiotics (Chloramphenicol, Kanamycin, and Ampicillin) were added into the bacterial solution to reach increasing concentrations of 0.5, 1, 5, 10, 50 μg/mL. Each plate contained two repeats of the same concentration. Controls without antibiotics and one blank with only the Modified M9 minimal growth medium were also prepared.

### 2.8 Imaging of *E.coli* growth

Fluorescence images of the samples in the cuvettes and in the culture plates were taken by a smartphone (Google Nexus 5) by placing samples on a Safe Imager™ 2.0 Blue Light Transilluminator (LIfeTechnologies) (excitation at 470nm).

## 3. Results and Discussion

### 3.1 Synthesis of fluoresceininamine (FA) pH-sensitive nanoparticles

Fluoresceininamine was selected as a pH-sensitive molecule because it has an intense absorption band in the visible. Even though it can adopt four different forms (dianion, anion, neutral and cation) depending on the pH, it is only highly fluorescent in its dianionic form(Sjöback et al., 1995). Furthermore, the $pK_a$ of the anion/dianion couple is about 6.4, which is suitable to measure changes in pH in biological media. The grafting of amino-functionalized molecules on carboxylic groups is a standard procedure (Montalbetti and Falque, 2005). The functionalization of PSNPs with fluoresceinamine (FA) was performed at pH=8 and 4 °C. The grafting of FA on PSNP1 and PSNP2 was carried out using 0.5 and 1 equivalent of FA per acrylic acid unit, respectively (**Scheme S2**). In all cases, the grafting did not change the hydrodynamic diameter of the nanoparticles significantly. The hydrodynamic of the fluoresceinamine conjugated nanoparticles (FANPs) remains around 60-70 nm (S1.3 and **Table S2**).

### 3.2 Spectroscopic properties of the FANPs

Absorption and fluorescence spectroscopy analysis of FANP1 and FANP2 are shown in **Figure S1**, their main spectroscopic data are given in **Table S2**. The particle suspensions have a maximum absorption at 488 and 490 nm and a maximum fluorescence emission at 519 and 521 nm in FANP1 and FANP2 respectively, in water at pH 8. There is a slight red shift compared to the free FA dye (Sjöback et al., 1995) which may come from the change of the local environment of the dye. The fluorescence quantum yield of the nanoparticles is between 12% and 14% for both particles at pH 8. This is lower than the free fluorescein amide dye (pH > 7, $\Phi_F$ = 79% (Munkholm et al., 1990)) which may be due to the formation of FA aggregates in the shell. The number of grafted fluorescein molecules is 530 and 340 for FANP1 and FANP2 respectively as estimated from the absorption spectra (Carvell et al., 1998).

The spectroscopic behaviour of these FA-grafted nanoparticles was then studied at various pH values (**Figure 1 and Figure S2**). The fluorescence spectra at pH=8 for FANP1 (**Figure 1A**) and FANP2 (**Figure 1C**) have a main band centred at 519 nm and 521 nm respectively. This main band was attributed to fluoresceinamide. The fluorescence spectra were then recorded at different pH (phosphate/citrate buffers 1mM in 140mM NaCl). Upon a decrease in the pH, the spectral intensity decreased both in the absorbance and fluorescence for FANPs. This behaviour is similar to that of fluorescein

in water. Moreover the pKa was determined from the fluorescence spectra using the Henderson-Hasselbalch equation:

$$I = \frac{I_A + I_B K_a 10^{pH}}{1 + K_a 10^{pH}}$$

Where I is the fluorescence intensity of the sample and $I_A$ and $I_B$ are the fluorescence intensities in the acidic and basic forms respectively (Valeur, 2001). The pKa for both types of nanoparticles is around 6.5 and a linear dependence of the fluorescence intensity was observed between pH 5.5 and 7.5. Both the pKa and the linear range are in agreement with the one of the free FA dye (Duong et al., 2006), therefore it seems that the grafting does not change the pH dependent fluorescent properties of FA. This is the useful pH range for the study of most biological systems. Compared to other approaches reported previously (Badugu et al., 2008; Wang et al., 2013), in this case the linearity of the signal covers a wider and more suitable range of pH values for detecting bacterial growth. The amplitude of the fluorescence intensity change between these two pH values is around 7-fold which is 3 times higher than previously reported (Wang, F. et al., 2014; Wang, X. et al., 2013). These properties will thus allow a sensitive and precise determination of the change in pH in biological systems.

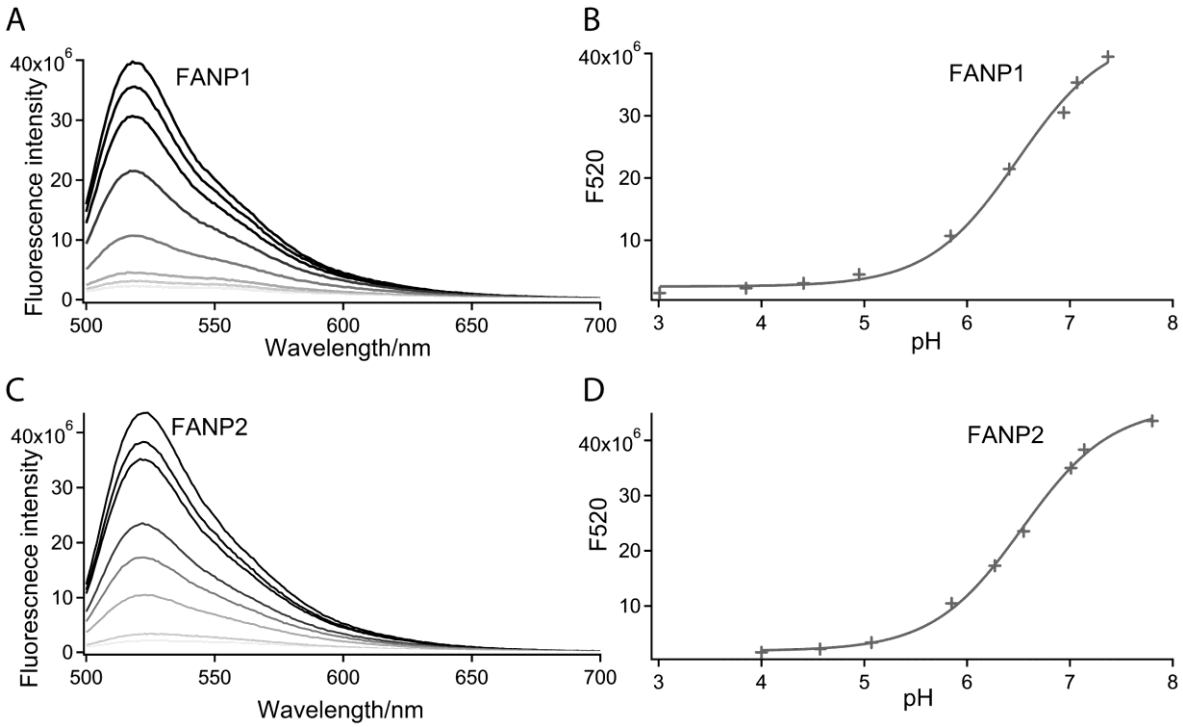


**Figure 1.** Fluorescence emission spectra of FANP1 (A) and FANP2(C) as a function of pH

($\lambda_{exc}$=495nm; phosphate/citrate buffer 1mM and 140mM NaCl). (B) Change in fluorescence intensity of FANP1 at 520nm as a function of pH. The data was fit using the Henderson-Hasselbalch equation with pKa=6.49. pH values: 7.37, 7.07, 6.94, 6.41, 5.84, 4.95, 4.41, 3.85, 3.01. (D) Change in fluorescence intensity of FANP2 at 520nm as a function of pH. The data was fit using the Henderson-Hasselbalch equation with pKa=6.53. pH values: 7.80, 7.14, 7.01, 6.55, 6.27, 5.85, 5.07, 4.57, 4.00.

### 3.3 Toxicity assessments of FANPs on *E.coli*

In order to assess the toxic effect of FANPs on *E.coli*, the growth rate of bacteria in the presence of FANPs was compared with the growth rate of *E.coli* bacteria alone. The growth rate was measured by absorbance measurement (OD@600nm) in a 96-well plate reader. The FANPs concentrations used were $8.2x10^{-7}$M, $4.1x10^{-7}$M and $8.2x10^{-8}$M.

*E.coli* bacteria with different concentrations FANP1 or FANP2 were incubated in the plate reader at 37°C in the dark overnight. A control with only bacteria was also prepared. Every 6 minutes the growth rate of the cells was monitored by measuring the optical density at 600nm by the plate reader **(Figure 2**, **Figure S3**). For an incubation of over ten hours the growth curves of bacteria with FANPs at different concentrations were practically the same as the growth curve of bacteria alone. This means that FANPs have no toxicity effect on bacterial growth in a long time scale independently of the kind of shell present on the FANPs.

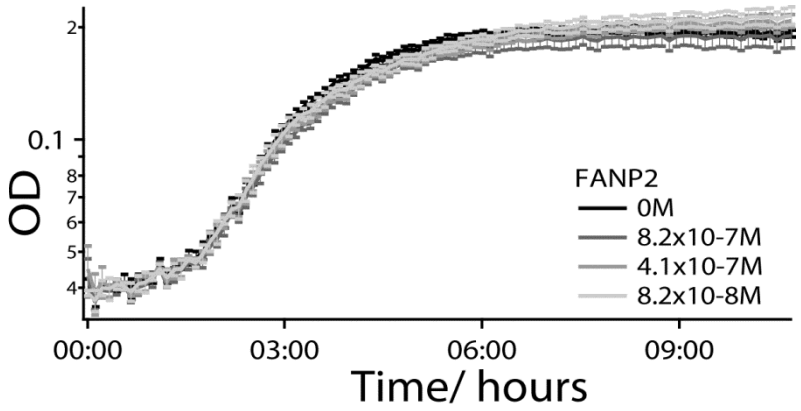


**Figure 2.** Growth curves of *E.coli* bacteria alone and of *E.coli* bacteria incubated with FANP2 particles at $8.2x10^{-7}$M, $4.1x10^{-7}$M and $8.2x10^{-8}$M. The error bars indicate the difference between the three replicates in the experiment.

### 3.4 Real-time detection of *E.coli* growth

Growth of *E.coli* bacteria with glucose results in the production of $CO_2$ and acetic acid and, therefore, in a decrease in pH of the growth medium. These FANPs have been shown to be photostable and the pH-dependent fluorescence change reversible (Detailed information in Supplemental Information S1.5 and S2.2). These unique features are very important for continuous monitoring for real-time detection of bacterial growth on long time scales. We thus tested whether they could be used to precisely monitor the pH change due to bacterial growth. In order to measure the change in fluorescence intensity of FANPs in the presence of *E.coli* bacteria, the growth medium with an initial pH of 7.0 and an initial *E.coli* bacterial concentration of $2x10^7$ CFU/mL(OD=0.25) was placed inside a cuvette in the presence of FANPs and were incubated at 37°C in the dark. Every 30 minutes the growth of the cells was monitored by measuring the optical density at 600 nm using a spectrophotometer (**Figure 3C, Figure S7C**). When the bacteria began to grow, the pH of the growth medium started to decrease. The pH of the samples was monitored at several time intervals with a pH meter. When the bacterial concentration increased to $1.1x10^8$CFU/mL (OD=1.1), the pH of the growth medium decreased to 5.8. At the same time, the emission spectra of the samples were measured. As bacterial growth increased the fluorescence intensity of both FANPs decreased significantly (**Figure 3A and Figure S7A**).

The fluorescence intensity of FANP2 for example decreased more than 80% during bacterial growth. Thanks to the calibration curve (**Figure 1D**) the pH can be evaluated by recording the change in fluorescence intensity of FANP2 in the growth medium (**Figure 3B**). It was found that these pH values were in full agreement with those measured by a pH meter (**Figure 3C**). Incubating FANP1 with *E.coli* gave similar results as those obtained with FANP2 (**Figure S7**). In conclusion, the pH-sensitive nanoparticles can be used to precisely monitor the pH variation due to bacterial growth (**Figure 3, Figure S7**).

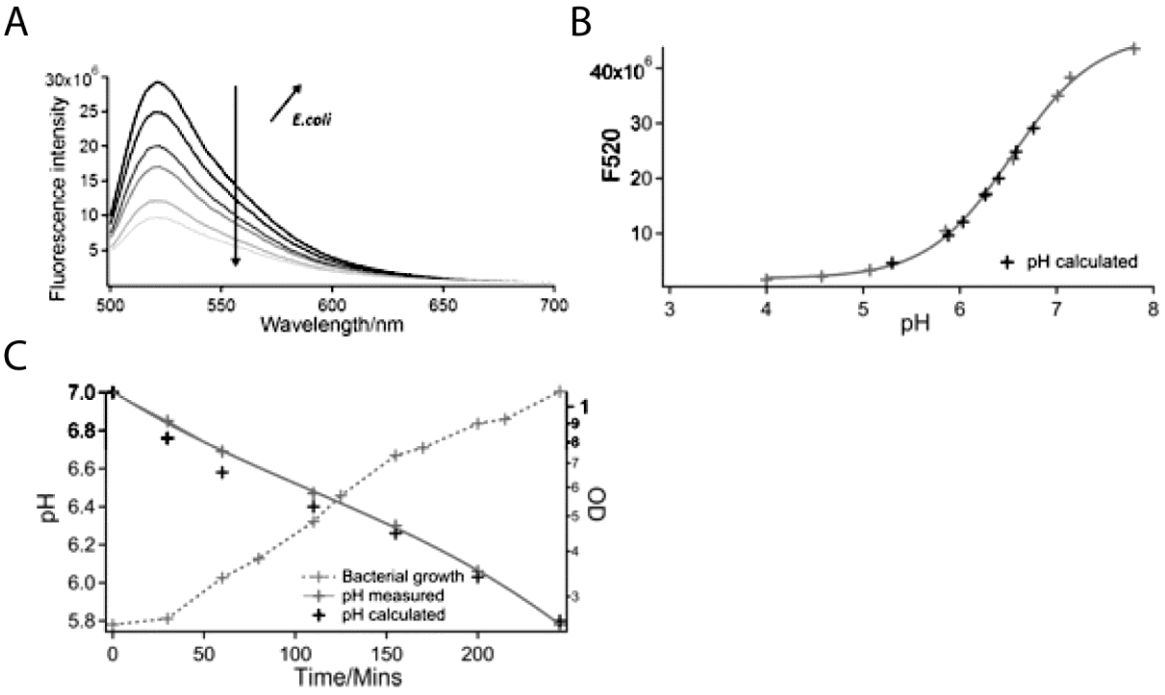


**Figure 3. (**A) Change in the fluorescence emission spectra of FANP2 with bacterial growth ($\lambda_{exc}$=495nm; Modified M9 Minimal Medium). (B) Change in fluorescence intensity of FANP2 at 520 nm and corresponding pH of the growth medium calculated by the Henderson-Hasselbalch equation. (C) Real-time bacterial growth curve (dotted line) and the corresponding pH evolution as measured by a pH meter (grey line) and the pH change calculated by the Henderson-Hasselbalch equation from the change in fluorescence (black crosses).

### 3.5 Sensitivity assessments

A successful pH nano-sensor for the detection of *E.coli* growth should be both rapid and sensitive to small changes in bacterial concentrations. We therefore performed assays in order to assess the sensitivity of FANPs compared with the one of the same concentration of free fluoresceinamine (FA) molecules using a lower starting concentration of bacteria. FANP1, FANP2 or FA molecules were added to the growth medium with an initial concentration of *E.coli* bacteria of $1x10^5$ CFU/mL (estimated OD= 0.001, measured OD=0.003-0.006) inside a cuvette and were incubated at 37°C in the dark. Every 30 minutes the growth of the cells was monitored by using a spectrophotometer (**Figure 4**). At the same time, the emission spectra of the samples were measured. The corresponding decrease in the percentage of the fluorescence intensity of FA molecules, FANP1 and FANP2 as a function of time is shown in **Figure 4**.

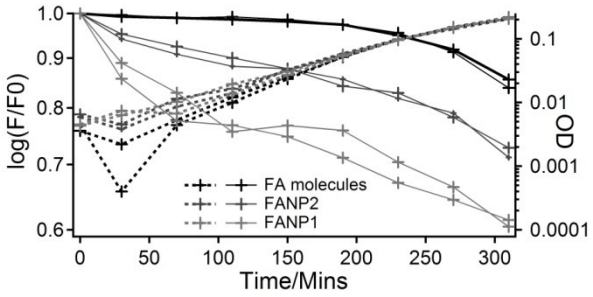


**Figure 4.** Measurement of *E.coli* bacteria growth incubated with FA molecules (black lines), FANP1 (light grey lines) and FANP2 (dark grey lines) using either the measurement of OD@600nm (dotted lines) or the % decrease in fluorescence intensity (full lines) as a function of time for FA molecules, FANP1 and FANP2. The two lines represent the replicates within the experiment.

It was found that there is almost no decrease in the fluorescence intensity of FA molecules until after more than 3 hours of bacterial growth. After about 5 hours, the fluorescence intensity of FA molecules decreased up to 15% (**Figure 4**, **Figure S8A, B**).

However, for the FANP2, the fluorescence intensity decreases up to 10% during the first hour of bacterial growth. The fluorescence intensity of FANP2 continually dropped to more than 30% (**Figure 4**, **Figure S8C, D**) over the five hours of the experiment. Hence, compared with a pH molecular sensor, such as FA, FANP2 is more sensitive, especially in the presence of a lower amount of bacteria as in the beginning of the experiment.

This difference is probably due to the high density of the sensing dyes at the surface of the nanoparticles. In solution a proton changes the fluorescence of one FA molecule whereas when a FA molecule is quenched by a proton within a FANP, it can in turn also act as a quencher, through energy transfer, to its unprotonated neighboring FAs. Indeed the emission spectrum of unprotonated FA (donor) overlaps with the absorption spectrum of protonated FA (acceptor) (Figure S14). Thus a single proton is likely to result in the quenching of several grafted FA (compared to only one in solution). This amplification can explain why FANPs are more sensitive than FA molecules to changes in pH.

Furthermore, the FANP1 appeared to be more sensitive than FANP2 in detecting the growth of *E.coli* bacteria. Indeed, during the first hour of bacterial growth, the fluorescence intensity of FANP1 continually decreased by almost 20% which is twice as much compared with FANP2 (**Figure 4**). Until 3 hours the fluorescence intensity of FANP1 decreased more than 30%, and at the end of the experiment it had decreased up

to 40% (**Figure 4**, **Figure S8E, F**). The difference between the two FANPs is probably due to the different number of FA grafted on FANP1 and FANP2. Indeed FA is more concentrated in FANP1 than FANP2 (530 FA per FANP1 and 340 FA per FANP2- Table S2). Thus the mean distance between two grafted FA is shorter in FANP1 compared to FANP2. As discussed above, FRET is likely to occur between unprotonated FA (donor) and protonated FA (acceptor). Energy transfer is distance dependent, thus it will be more efficient in FANP1 than FANP2.

As mentioned above, the growth of the cells was monitored using a spectrophotometer that reads the optical density (OD@600nm) of the samples every 30 minutes (**Figure 4**). From the time at which the bacteria started to grow until two hours of growth, it was found that this small amount of bacteria couldn't be measured accurately the change in optical density. In addition, there were large fluctuations in the signal in the first hour of growth, and as the bacterial number increased, the measurements of spectrophotometers became more reproducible. However, as shown in **Figure 4**, the fluorescence intensity measurements from the FANP1 and FANP2 particles are very reliable and reproducible from the very beginning until the end of the experiments. In addition a similar experiment with bacteria at an initial OD of 0.00001 incubated with FANP2 particles was performed (Supplemental Information S2.3). Figure S13 shows that the measurements of OD from spectrometers are not sensitive enough in the early stages of growth, however as long as there is metabolism of *E.coli* bacteria, the pH-sensitive nanoparticles are able to detect it. These results show that these pH-sensitive nanoparticles are not only more sensitive than a molecular sensor such as the FA molecules but also more sensitive than typical OD measurements.

### 3.6 Screening of cell growth in a 96 well plate

Since the FANPs can be used to measure the change in pH resulting from the metabolic activity of live bacteria, they can be used to discriminate whether the bacteria have died or have a decreased growth rate due to the fluorescence intensity change caused by metabolism. This approach can thus be more sensitive compared with typical OD meters and can be performed in complex media. We next tested the potential ability of FANPs for high-throughput screening of *E.coli* bacteria.

In order to measure the fluorescence evolution of FANPs when incubated with smaller volumes of bacteria, *E.coli* were incubated in a 96-well plate with different concentrations ($8.2 \times 10^{-7}$M, $4.1 \times 10^{-7}$M and $8.2 \times 10^{-8}$M) of FANP1 or FANP2 and placed

in a plate reader at 37°C in the dark overnight. A control with bacteria without nanoparticles was also prepared. The fluorescence intensity of each well was monitored every 6 minutes by using a F485/14 filter for excitation and a F535/40 filter for emission (**Figure S9**).

The fluorescence of FANPs was measured during the growth of *E.coli* for over ten hours. The fluorescence intensity of FANP1 decreased simultaneously with *E.coli* growth (**Figure S9A**). Comparison of the three different concentrations of FANP1 used shows that the response is independent of the amount of FANP1 present **(Figure S9B)**. Using FANP2 to measure the growth of *E.coli* gave very similar results as those obtained with FANP1 (**Figure S9C, D**). The correlation between the $OD_{600}$ and the fluorescence of FANPs is shown in **Figure S10**. One can see that the change in fluorescence of FANPs as a function of the growth of bacteria shows a good correlation with the OD ($r^2$=0.94 for FANP1 and 0.93 for FANP2) over 15 hours of continuous measurements which is a significantly improved correlation compared with a previous report using acridine orange (Pak et al., 2013).

As described above, the amount of FANP used in the cuvette experiments for sensitivity assessments was $8.2x10^{-7}$M. Screening of bacterial growth in a 96 well plate with different FANP concentrations ($8.2x10^{-7}$M, $4.1x10^{-7}$M and $8.2x10^{-8}$M) shows that even after a ten-fold decrease in the concentration of FANP ($8.2x10^{-7}M \rightarrow 8.2x10^{-8}$M), one can still detect bacterial growth rapidly and accurately. Because of their stability and sensitivity these FANPs could be used as a novel indicator for screening of potential growth inhibition experiments.

### 3.7 High-throughput screening of bacterial growth inhibition by antibiotics

After demonstrating that FANPs can be used for measurement of *E.coli* bacteria growth in small volumes, we wanted to determine whether this approach could be used for high throughput experiments such as the detection of antibiotic resistance. In order to compare the results obtained by the change in OD with the change in fluorescence of FANPs ($8.2x10^{-8}$M) the effects of several common antibacterial drugs (Chloramphenicol, Kanamycin, and Ampicillin) on bacteria growth and metabolism were measured. The concentration of antibiotics used were 0.5, 1, 5, 10, 50 μg/mL, which cover the range of the known recommended concentrations of these antibiotics. The inhibitory effect of these drugs on the growth of *E.coli* as measured by the increase of the OD or the decrease in fluorescence of FANP1 is shown in **Figure 5**.

When increasing the concentration of antibiotics, the growth rate of *E.coli* bacteria decreases as measured by OD (**Figure 5A, C, E**). At the same time, the fluorescence intensity of FANP1 decreases at a slower rate when increasing the dose of the drugs (**Figure 5B, D, F**).

Moreover, from the growth curve, one can notice that after about ten hours of incubation bacterial growth reached the stationary phase, as measured by the OD, indicating that cell growth slowed down and that bacteria grew and died at the same rate, resulting in a constant number of bacteria. However, by measuring the OD it is not possible to measure the presence of bacterial growth once the population has reached stationary phase. On the other hand, the increase in the change in fluorescence at these later time points allows for a measurement of the amount of ongoing metabolism of *E.coli*. The same results were obtained for FANP2 (**Figure S11**). As anticipated, reducing the dose of antibiotics reduces its inhibitory effect, and the changes in cell metabolism can be measured reliably and accurately by using FANPs.

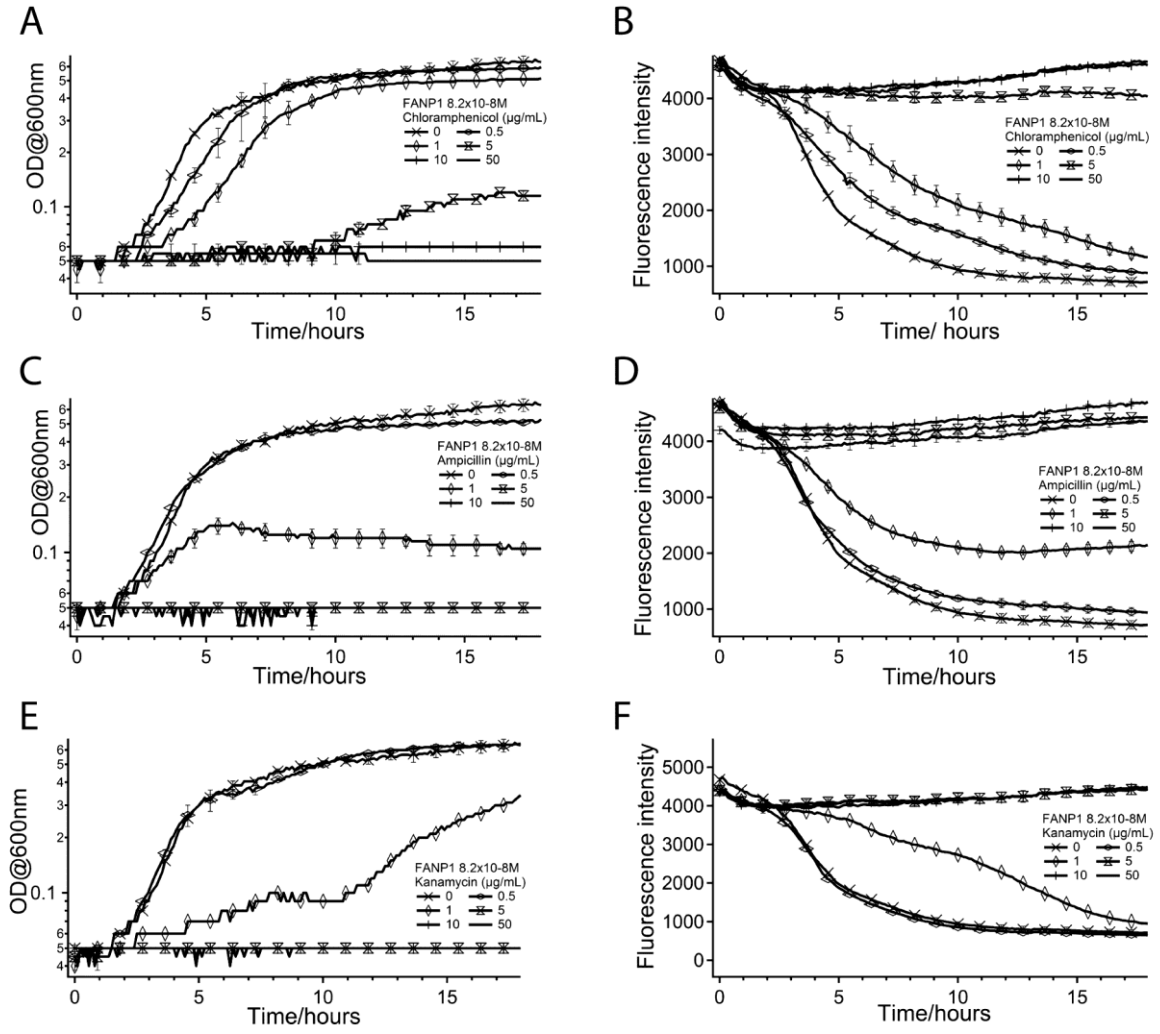

**Figure 5.** The inhibitory effect of three antibiotics on the growth of bacteria: Chloramphenicol (A,B), Kanamycin (C,D), and Ampicillin (E,F) at different concentration (0.5, 1, 5, 10, 50 µg/mL). The change in the growth of *E.coli* was measured by an increase of the OD (A, C, E) and by a decrease of fluorescence of FANP1 (B, D, F). The error bars indicate the difference between the three replicates in the experiment.

### 3.8 Imaging of *E.coli* growth

FANP1 and FANP2 were added to the growth medium with an initial concentration of *E.coli* of 3-6x$10^5$ CFU/mL (OD=0.003-0.006) inside a cuvette (**Figure 6A a0, c0**). After an overnight incubation, the fluorescence intensity of the cuvettes with bacteria decreased significantly (**Figure 6A a1, c1**) and the decrease could be easily seen by eye with the help of a lamp (exc@470nm). However, the fluorescence intensity of the cuvettes without bacteria remains unchanged (**Figure 6A b0, b1, d0, d1**).

In order to test whether these FANPs could be used to monitor bacterial growth on a solid support, they were embedded in agar with growth medium, as used traditionally to follow the formation of bacterial colonies.

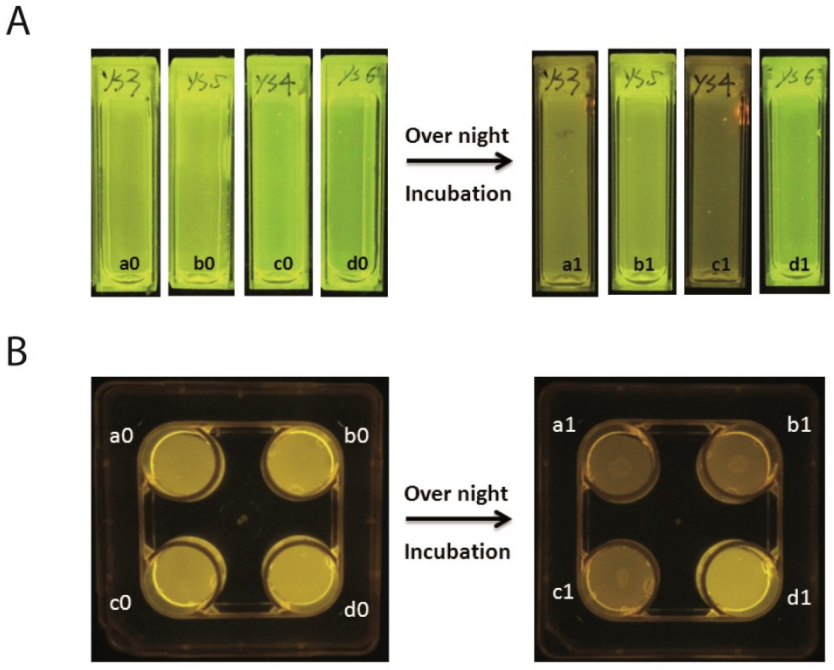


**Figure 6**. A: a0, c0: FANP1 and FANP2 in growth medium with an initial concentration of *E.coli* of 3x$10^5$CFU/ml (OD=0.003). b0 and d0: FANP1 and FANP2 in growth medium. a1, b1, c1, d1 are fluorescence images of a0, b0, c0, d0 after one night incubation (37°C). B: Fluorescence images of bacterial growth on FANP2 agarose (a0, b0, c0), compared to fluorescence images of FANP2 agarose alone (d0). a1, b1, c1, d1 are fluorescence images of a0, b0, c0, d0 after one night incubation (37°C).

As shown in **Figure 6B** and **Figure S12**, the pH-sensitive cell culture plates initially display a homogeneous yellow-green fluorescence, indicating a starting pH

value of 6.8. After an overnight growth of bacteria it can be seen that significant acidification of the whole agarose layer has occurred. Even if the initial localizations of bacterial solutions are different, the protons produced by the bacteria during growth have caused a global influence on the particles in the agarose as the fluorescence intensity of the whole surface is strongly reduced. This result indicates that these particles could be used to screen for bacteria that grow selectively on solid media.

## 4. Conclusions

The novel pH-sensitive nanoparticles described herein have distinct features that make them suitable for the development of biosensors including brightness, stability in growth medium, non-toxicity, high water solubility, high sensitivity, and ease of bioconjugation and incorporation into a biocompatible matrix. They can rapidly and accurately detect bacterial growth by detecting the change of pH resulting from cellular metabolism. Due to the brightness of these nanoparticles, they could be used to develop new systems for quantitative biosensor applications for microfluidic devices. One of the important advantages of this approach is that a change in pH can be easily monitored either by a simple change in fluorescence at a specific wavelength or even by eye, for a qualitative result in either a liquid or solid support. These FNAPs can be easily synthesized with low cost and can be used in any laboratory without additional expensive instruments or operators. Moreover, these particles allow for continuous monitoring for long time scale experiments and can be used to monitor a large number of samples for high-throughput screening applications. For example they can be used to measure the metabolic activities of bacteria as an indicator of their susceptibility to antibacterial drugs, as shown here, or for the screening and discovery of novel growth inhibitors. These particles could also be used to study the change in metabolism in different biological systems such as during the formation of biofilms (Vroom et al., 1999), in the event of skin infections (Valdés et al., 2012) or even to detect the presence of tumour cells during surgery due to their acidic environment (Pellegrini et al., 2014).

## Acknowledgements

Financial support for this work was provided by the CNRS (Centre National de la Recherche Scientifique) of France – Interface Physique Chimie Biologie Soutien à la prise de risque- and by Institut d'Alembert (FR 3242 CNRS- ENS de Cachan). A PhD

grant for Y.S. was provided by the MENESR (Ministère de l'Education Nationale, de l'Enseignement Superieur et de la Recherche) of France.

## References

Adams, L.K., Lyon, D.Y., McIntosh, A., Alvarez, P.J.J., 2006. Water Sci. Technol. J. Int. Assoc. Water Pollut. Res. 54, 327–334.

Agayn, V.I., Walt, D.R., 1993. Biotechnol. Nat. Publ. Co. 11, 726–729.

Badugu, R., Kostov, Y., Rao, G., Tolosa, L., 2008. Biotechnol. Prog. 24, 1393–1401.

Barker, L.M., Nanassy, O.Z., Reed, M.W., Geelhood, S.J., Pfalzgraf, R.D., Cangelosi, G.A., De Korte, D., 2010. Transfusion (Paris) 50, 2731–2737.

Boissé, S., Rieger, J., Belal, K., Di-Cicco, A., Beaunier, P., Li, M.-H., Charleux, B., 2010. Chem. Commun. 46, 1950.

Carvell, M., Robb, I.D., Small, P.W., 1998. Polymer 39, 393–398.

Chalova, V., Woodward, C. l., Ricke, S. c., 2003. J. Rapid Methods Autom. Microbiol. 11, 313–324.

Chang, W.-H., Wang, C.-H., Lin, C.-L., Wu, J.-J., Lee, M.S., Lee, G.-B., 2015. Biosens. Bioelectron. 66, 148–154.

Chen, Z.-Z., Cai, L., Chen, M.-Y., Lin, Y., Pang, D.-W., Tang, H.-W., 2015. Biosens. Bioelectron. 66, 95–102.

Chunglok, W., Wuragil, D.K., Oaew, S., Somasundrum, M., Surareungchai, W., 2011. Biosens. Bioelectron. 26, 3584–3589.

Duong, H.D., Sohn, O.-J., Lam, H.T., Rhee, J.I., 2006. Microchem. J. 84, 50–55.

Farris, L., Habteselassie, M.Y., Perry, L., Chen, Y., Turco, R., Reuhs, B., Applegate, B., 2008. Luminescence Techniques for the Detection of Bacterial Pathogens, in: Zourob, M., Elwary, S., Turner, A. (Eds.), Principles of Bacterial Detection: Biosensors, Recognition Receptors and Microsystems. Springer New York, pp. 213–230.

Gasol, J.M., Zweifel, U.L., Peters, F., Fuhrman, J.A., Hagström, Å., 1999. Appl. Environ. Microbiol. 65, 4475–4483.

Gopinath, S.C.B., Tang, T.-H., Chen, Y., Citartan, M., Lakshmipriya, T., 2014. Biosens. Bioelectron. 60, 332–342.

Grazon, C., Rieger, J., Méallet-Renault, R., Clavier, G., Charleux, B., 2011. Macromol. Rapid Commun. 32, 699–705.

Gunaydin, E., Eyigor, A., Carli, K.T., 2007. Lett. Appl. Microbiol. 44, 24–29.

Hassan, A.-R.H.A.-A., de la Escosura-Muñiz, A., Merkoçi, A., 2015. Biosens. Bioelectron., Special Issue: BIOSENSORS 2014 67, 511–515.

Huang, Y., Sudibya, H.G., Chen, P., 2011. Biosens. Bioelectron. 26, 4257–4261.

Jain, S., Chattopadhyay, S., Jackeray, R., Abid, C.K.V.Z., Kohli, G.S., Singh, H., 2012. Biosens. Bioelectron. 31, 37–43.

John, G.T., Goelling, D., Klimant, I., Schneider, H., Heinzle, E., 2003. J. Dairy Res. 70, 327–333.

Ko, S., Gunasekaran, S., Yu, J., 2010. Food Control 21, 155–161.

Lazcka, O., Del Campo, F.J., Muñoz, F.X., 2007. Biosens. Bioelectron. 22, 1205–1217.

Martens-Habbena, W., Sass, H., 2006. Appl. Environ. Microbiol. 72, 87–95.

Montalbetti, C.A.G.N., Falque, V., 2005. Tetrahedron 61, 10827–10852.

Mouffouk, F., da Costa, A.M.R., Martins, J., Zourob, M., Abu-Salah, K.M., Alrokayan, S.A., 2011. Biosens. Bioelectron. 26, 3517–3523.

Munkholm, C., Parkinson, D.R., Walt, D.R., 1990. J. Am. Chem. Soc. 112, 2608–2612.

Nayak, M., Kotian, A., Marathe, S., Chakravortty, D., 2009. Biosens. Bioelectron. 25, 661–667.

Noble, R.T., Weisberg, S.B., 2005. J. Water Health 3, 381–392.

Pak, D., Koo, O.K., Story, R.S., O'Bryan, C.A., Crandall, P.G., Lee, S.-O., Ricke, S.C., 2013. J. Environ. Sci. Health B 48, 512–515.

Palavecino, E.L., Yomtovian, R.A., Jacobs, M.R., 2006. Clin. Lab. 52, 443–456.

Pellegrini, P., Strambi, A., Zipoli, C., Hägg-Olofsson, M., Buoncervello, M., Linder, S., De Milito, A., 2014. Autophagy 10, 562–571.

Pourciel-Gouzy, M.L., Sant, W., Humenyuk, I., Malaquin, L., Dollat, X., Temple-Boyer, P., 2004. Sens. Actuators B Chem., The 17th Euopean Conference on Solid-State Transducers, University of Minho, Guimares, Portugal, September 21-24, 2003 103, 247–251.

Seo, S.-H., Lee, Y.-R., Ho Jeon, J., Hwang, Y.-R., Park, P.-G., Ahn, D.-R., Han, K.-C., Rhie, G.-E., Hong, K.-J., 2015. Biosens. Bioelectron. 64, 69–73.

Sjöback, R., Nygren, J., Kubista, M., 1995. Spectrochim. Acta. A. Mol. Biomol. Spectrosc. 51, L7–L21.

Valdés, P.A., Leblond, F., Jacobs, V.L., Wilson, B.C., Paulsen, K.D., Roberts, D.W., 2012. Sci. Rep. 2.

Valeur, B., 2001. Molecular Fluorescence. Wiley-VCH Verlag GmbH.

Vroom, J.M., De Grauw, K.J., Gerritsen, H.C., Bradshaw, D.J., Marsh, P.D., Watson, G.K., Birmingham, J.J., Allison, C., 1999. Appl. Environ. Microbiol. 65, 3502–3511.

Wang, F., Raval, Y., Chen, H., Tzeng, T.-R.J., DesJardins, J.D., Anker, J.N., 2014. Adv. Healthc. Mater. 3, 197–204.

Wang, S., Lawson, R., Ray, P.C., Yu, H., 2011. Toxicol. Ind. Health 27, 547–554.

Wang, X., Meier, R.J., Wolfbeis, O.S., 2013. Angew. Chem. Int. Ed. 52, 406–409.

Wang, Y., Ye, Z., Ying, Y., 2012. Sensors 12, 3449–3471.

Wan, Y., Sun, Y., Qi, P., Wang, P., Zhang, D., 2014. Biosens. Bioelectron. 55, 289–293.

Washington, J.A., 1996. Principles of Diagnosis, in: Baron, S. (Ed.), Medical Microbiology. University of Texas Medical Branch at Galveston, Galveston (TX).

Young, O.A., Thomson, R.D., Merhtens, V.G., Loeffen, M.P.F., 2004. Meat Sci. 67, 107–112.

Zlitni, S., Blanchard, J.E., Brown, E.D., 2009. Methods Mol. Biol. Clifton NJ 486, 13–27.

## Highlights :

1. Two highly water-soluble, biocompatible, stable and bright fluoresceinamine based pH-sensitive nanoparticles (FANPs) are presented.
2. These FANPs can be used for a rapid, accurate, reproducible and highly sensitive detection of *E.coli* bacterial growth.
3. These FANPs are very easy and to synthesize with a low cost and can be easily used in any laboratory without additional expensive instrumentation or experienced operators.
4. These FANPs allow for continuous monitoring for real-time detection of bacterial growth and can be used for screening of a large number of samples for high-throughput applications such as the measurement of the change in bacterial metabolism due to the presence of antibiotics.

### Figure legends

**Figure 1.** Fluorescence emission spectra of FANP1 (A) and FANP2(C) as a function of pH ($\lambda_{exc}$=495nm; phosphate/citrate buffer 1mM and 140mM NaCl). B: Change in fluorescence intensity of FANP1 at 520nm as a function of pH. The data was fit using the Henderson-Hasselbalch equation with pKa=6.49. pH values: 7.37, 7.07, 6.94, 6.41, 5.84, 4.95, 4.41, 3.85, 3.01. D: Change in fluorescence intensity of FANP2 at 520nm as a function of pH. The data was fit using the Henderson-Hasselbalch equation with pKa=6.53. pH values: 7.80, 7.14, 7.01, 6.55, 6.27, 5.85, 5.07, 4.57, 4.00.

**Figure 2.** Growth curves of E.coli bacteria alone and of E.coli bacteria incubated with FANP2 particles at $8.2x10^{-7}$M, $4.1x10^{-7}$M and $8.2x10^{-8}$M. The error bars indicate the difference between the three replicates in the experiment.

**Figure 3.** A: Change in the fluorescence emission spectra of FANP2 with bacterial growth ($\lambda_{exc}$=495nm; Modified M9 Minimal Medium). B: Change in fluorescence intensity of FANP2 at 520nm and corresponding pH of the growth medium calculated by the Henderson-Hasselbalch equation. C: Real-time bacterial growth curve (dotted line) and the corresponding pH evolution as measured by a pH meter (grey line) or the corresponding pH change calculated by the Henderson-Hasselbalch equation from the change in fluorescence (black crosses).

**Figure 4.** Measurement of *E.coli* bacteria growth incubated with FA molecules (black lines), FANP1 (light grey lines) and FANP2 (dark grey lines) using either the measurement of OD@600nm (dotted lines) or the decrease (%) of fluorescence intensity (full lines) as a function of time for FA molecules, FANP1 and FANP2. The two lines represent the replicates within the same experiment. Each experiment was repeated twice.

**Figure 5.** The inhibitory effect of three antibiotics on the growth of bacteria: Chloramphenicol (A,B), Kanamycin (C,D), and Ampicillin (E,F) at different concentration (0.5, 1, 5, 10, 50 µg/mL). The change in the growth of *E.coli* was measured by an increase of the OD (A, C, E) and by a decrease of fluorescence of FANP1 (B, D, F).

**Figure 6**. A: a0, c0: FANP1 and FANP2 in growth medium with an initial concentration of *E.coli* of $3x10^5$CFU/ml (OD=0.003). b0 and d0: FANP1 and FANP2 in growth medium. a1, b1, c1, d1 are fluorescence images of a0, b0, c0, d0 after one night incubation (37°C). B: Fluorescence images of bacterial growth on FANP2 agarose (a0, b0, c0), compared to fluorescence images of FANP2 agarose alone (d0). a1, b1, c1, d1 are fluorescence images of a0, b0, c0, d0 after one night incubation (37°C).